Physics of selective conduction and point mutation in biological ion channels

W.A.T. Gibby,[1,*] M.L. Barabash,[1] C. Guardiani,[1,2] D. G. Luchinsky,[1,3,†] and P.V.E. McClintock[1,‡]

[1] *Department of Physics, Lancaster University, Lancaster LA1 4YB, UK.*
[2] *Department of Mechanical and Aerospace Engineering, Sapienza University, Rome, Italy*
[3] *KBR, Inc., Ames Research Center, Moffett Field, CA, USA*

(Dated: April 23, 2021)

We introduce a statistical and linear response theory of selective conduction in biological ion channels with multiple binding sites and possible point mutation. We derive an effective grand-canonical ensemble and generalised Einstein relations for the selectivity filter, assuming strongly coordinated ionic motion, and allowing for ionic Coulomb blockade. The theory agrees well with data from the KcsA K^+ channel and a mutant. We show that the Eisenman relations for thermodynamic selectivity follow from the condition for fast conduction and find that maximum conduction requires the binding sites to be nearly identical.

Understanding, predicting and optimising the ionic transport properties of nanopores remains a critical challenge to both nanotechnology [1] and biophysics [2, 3]. Interest is partially motivated by the importance and diversity of the applications, including water purification [4], DNA sequencing [5], and biological ion channels together with their role in medicine [2, 6, 7].

Biological channels are proteins with central pathways (nanopores), spanning a lipid membrane. Their primary function of selectively conducting ions at nearly the diffusion rate is effected mainly by a narrow selectivity filter (SF) (Fig. 1). Key structural features of K^+ SFs, [2, 8, 9], include a sequence of sub-nanometer sized binding sites that can have strongly charged residues with site and ion-specific affinities.

Point mutations causing structural changes in the SF, and differences in the extended structure away from the SF, can greatly influence conduction and selectivity [10–15]. For example, K^+ channels have conserved SF sequences, and yet their conductance ranges from 5-270 pS [16]. Predicting these changes is a challenging problem. Nano-confinement of ions in the SF is affected by e.g. partial charges [17, 18], ionic diffusivity [19], electrical permittivity [20, 21], quantum mechanical interactions and polarisation [22–29], and the species-dependent positions of binding sites [25, 30–32].

Particularly intriguing problems associated with point mutations are understanding the relations between selectivity, conductivity [30–34], highly coordinated conduction mechanisms [35–42], and the occupancy of individual sites and of the SF as a whole. Useful insight clearly requires a fundamental theory.

Earlier statistical theories focused primarily either on the problem of selectivity, or on that of conductivity. Thermodynamic selectivity [43] in this context is defined as the difference between species of interaction energy between bulk and the channel. In K^+ channels it led to the snug-fit model highlighting the importance of close coordination of ions by charged oxygen atoms [35, 44]; and it has been analysed at the scale of individual binding sites in many channel types [45–49]. Ionic conduction occurs via a knock-on mechanism [36, 50–52], which has been investigated using statistical physics [53, 54] leading to an important analogy between ionic Coulomb blockade (ICB) and electronic Coulomb blockade in quantum dots [55–57] This, also highlighted the importance of long-range interactions for valence selectivity [55–61]. Furthermore, statistical and information theories have provided insight into the binding of ions and relationship with the potential of mean force [62–65].

These insightful theories have often ignored, however, the multi-component and multi-site nature of biological SFs and do not account for the ion-specific affinities of individual binding sites. A theory able to encompass these phenomena is crucial for understanding the properties of real SF's and might also illuminsted phenomena such as ICB [60, 61], anomalous mole fraction effect [66–68], and the mechanism of knock-on [14, 38], all of which are subjects of extensive debate.

In this Letter we introduce such a theory, based on statistical physics and linear response. It relates both the kinetic and thermodynamic properties of permeation directly to pore structure, and explicitly includes ionic correlations and knock-on conduction, from which we analytically derive Eisenman's selectivity relation. Furthermore, it allows one to calculate optimal transport parameters, and conductivities of individual sites and of the SF as a whole. It opens the way to statistical analyses of all narrow biological channels, including the effects of point mutation, and it provides the foundation for kinetic modeling to account for the dynamic effects of potential barriers and for selectivity. [32]

The K^+-conducting channel KcsA (Fig. 1) has a pore (c) of average radius R_c ∼2Å, length L_c ∼12Å , volume V_c, and 4 binding sites formed by charged oxygen atoms in carbonyl/hydroxyl groups [35, 36]. The pore is thermally and diffusively coupled to the left (L) and right (R) bulk reservoirs (b) (bottom and top respectively in Fig. 1(a)). Each bulk contains mixed solutions of S total ionic species where $s \in 1, \cdots, S$. The primary function of the pore is conduction of K^+ at close to the rate of

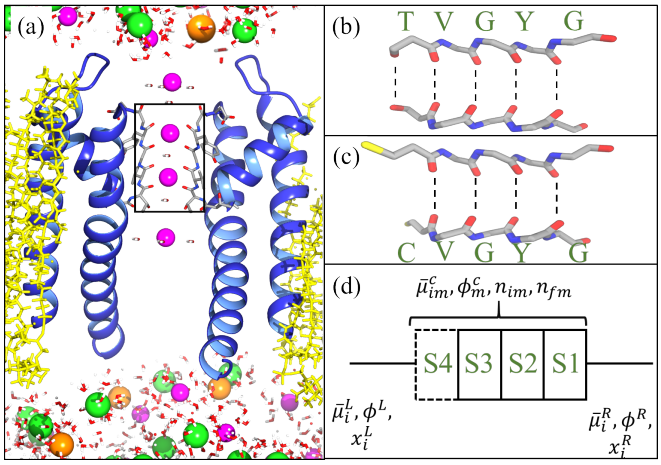

FIG. 1. Structure of open KcsA (5vk6.pdb) [69] visualised using chimera [70]. (a) Two chains (blue ribbons) spanning a lipid membrane (yellow strands) between two aqueous ionic solutions. The SF is located within the box, and K^+ (purple), Na^+ (orange), and Cl^- (green) ions alongside water molecules are included. (b) Structure of the SF for wild type KcsA and (c) the T75C mutant, with indicated amino acids at binding sites. (d) Lattice model used to define the system.

free diffusion whilst selecting strongly against Na^+.

The system as a whole is characterized by the canonical ensemble with constant total particle number N_s, volume V and temperature T. Ions are free to leave the bulk solution and bind at specific sites in the pore, with N_s^b being the total number of ions in either bulk prior to binding. Due to the narrowness of the pore, 1-dimensional ionic conduction occurs via a finite number of binding sites M. Each site $m \in 1, \cdots, M$ can hold a single ion at most, therefore, the total number of ions in the pore is $n = \sum_m^M \sum_s^S n_{sm} \leq M$, where $\sum_{s=1}^S n_{sm} \in 0, 1$ and $n_s = \sum_{m=1}^M n_{sm}$. All possible configurations of ionic binding $\{n_j\}$ are mutually exclusive leading to Fermi statistics [65]. Because we are interested in the statistical properties of the pore, we use an effective *grand canonical ensemble* (GCE), whose full derivation is provided in [71]. We start with the total energy of the system, found by explicitly counting the number of ions of each species that leave the left (n''_{sm}) and right (n'_{sm}) bulks and enter site m in the pore (keeping the total number of ions constant).

$$E(\{n_j\}) = E_0 + \mathcal{E}(\{n_j\}) + \sum_{s=1}^{S} \left(N_s^L - \sum_{m=1}^{M} n''_{sm} \right) \mu_s^L + \sum_{s=1} (N_s^R - \sum_{m=1}^{M} n'_{sm}) \mu_s^R + kT \ln(n_0)! + \sum_{s=1}^{S} kT \ln n_s! + \sum_{s=1}^{S} \sum_{m=1}^{M} (n'_{sm} + n''_{sm})(\bar{\mu}^c_{sm} + q z_s \phi^c_m). \quad (1)$$

Here we define the thermodynamic part of the energy $E_0 = TS - pV$, entropy S, pressure p, the long range interaction energy $\mathcal{E}$ between ions and fixed charges, and n_0 is the number of empty sites.

In (1), the bulk electrolytes and binding sites of the pore represent a system with several interpentrating solutions, each characterized by its own chemical potential. The electrochemical potential in the bulk is defined [64, 72, 73] as the sum of ideal, excess, and electrostatic parts

$$\mu_s^b = \mu_s^{0,b} + kT \ln \left(x_s^b \right) + \bar{\mu}_s^b + q z_s \phi^b, \quad (2)$$

where q, x_s^b, z_s, ϕ^b and $\bar{\mu}_s^b$ denote the unit charge, mole fraction, valence, external electric and excess chemical potential respectively. Term: $\mu_s^{0,b}$ corresponds to the thermal wavelength and internal partition function in the bulk.

For a binding site, the electrochemical potential [74]

$$\mu^c_{sm} = \mu_s^{0,c} + kT \ln[(n_s+1)/n_0] + \bar{\mu}^c_{sm} + q z_s \phi^c_m + \Delta\mathcal{E}, \quad (3)$$

is characterized by excess chemical $\bar{\mu}^c_{sm}$ and electrostatic $q z_s \phi^c_m$ potentials at each site, the change in the interaction energy between ions $\Delta\mathcal{E}$ when one ion is added to the pore, and the factor $kT \ln(n_s + 1)/n_0$ accounting for indistinguishably of ions in the pore. Term: $\mu_s^{0,c}$ corresponds to the thermal wavelength and internal partition function in the pore. We assume that $\mu_s^{0,c} = \mu_s^{0,b}$ and factor it out of our expression of total energy (1) For further details see [71]).

We note that ionic transition from the bulk to the pore results in small fluctuations of total energy (1). This allows us to derive [65, 75] the GCE for the pore by factorizing the partition function into bulk and pore constituents and cancelling constant terms

$$P(\{n_j\}) = \mathcal{Z}^{-1} \left(\frac{1}{n_0!} \prod_s^S \frac{1}{n_s!} \right) \times \exp \left[\left(\sum_{s=1}^{S} \sum_{m=1}^{M} n_{sm} \Delta\tilde{\mu}^b_{sm} - \mathcal{E}(\{n_j\}) \right) / kT \right] \quad (4)$$

with $\Delta\tilde{\mu}^b_{sm} = \Delta\bar{\mu}^b_{sm} + q z_s \Delta\phi^b_m + kT \log(x^b_s)$ and partition function $\mathcal{Z}$. Note that Δ is the difference between pore and bulk, so $\Delta\bar{\mu}^b_{sm} = \bar{\mu}^b_s - \bar{\mu}^c_{sm}$ etc.

The corresponding free energy ($G = E - TS + pV$) is,

$$G(\{n_j\}) = \mathcal{E}(\{n_j\}) + kT \ln n_0! + \sum_{s=1}^{S} kT \ln n_s! - \sum_{s=1}^{S} \sum_{m=1}^{M} n_{sm} [\Delta\bar{\mu}^b_{sm} + q z_s \Delta\phi^b_m + kT \ln(x^b_s)]. \quad (5)$$

The derived model is consistent with many earlier theoretical results [62, 64, 65, 76, 77] and accounts for key features of selective conduction in biological SF's, including ICB and structure of the individual SF sites.

The grand potential ($\Omega = -kT \ln \mathcal{Z}$) can now be used to compute the occupancies of the sites and the SF

$$\langle n_{sm} \rangle = \sum_{\{n_j\}} n_{sm} P(\{n_j\}) \qquad \langle n_s \rangle = \sum_m \langle n_{sm} \rangle. \tag{6}$$

These are used to calculate the conductivity σ_{sm} (defined via the static density susceptibility χ_{sm}, see Eq. (29) of [71]) at each site, and the total conductivity σ^T of the SF

$$\sigma_{sm} = z_s q^2 \chi_{sm} D_{sm}, \quad \sigma_s^T = \left(\sum_m^M \sigma_{sm}^{-1} \right)^{-1}, \tag{7}$$

where D_{sm} is the species diffusivity at site m. It is clear that, in general, local geometry influences directly the site conductivity. For single-file motion, conduction through sites of length L_{sm} and cross-sectional area A_{sm} connected in series (Fig. 1), the conductance $\mathcal{G}^T$ and total current across the pore are

$$I = \mathcal{G}^T \mathcal{V}, \quad \mathcal{G}^T = \sum_s^S \left(\sum_m^M \frac{L_{sm}}{A_{sm} \sigma_{sm}} \right)^{-1}. \tag{8}$$

To compare these results to experimental data, we consider conduction of the wild-type (WT) KcsA filter and its mutant T75C (MuT) obtained by point mutation [11] of site S4, see Fig. 1.

We assume that: bulk solutions contain Na^+ and K^+ at concentrations of 0.2M; ions may occupy neighbouring sites; and the SF occupancy is restricted to 3 ions. Under these plausible conditions there are 65 configurational states [71]. To estimate their energies $G(\{n_j\})$ we use Eqs. (4), (5) and approximate the total electrostatic energy of the pore $\mathcal{E}$ as a capacitor [55, 57–59] of capacitance C, total charge $Q = (n_f + \sum_s n_s)\, q$, and charging energy $U_c \sim 10kT$

$$\mathcal{E} = U_c \left[\sum_m \left(\sum_s n_{sm} + n_{fm} \right) \right]^2; \quad U_c = \frac{q^2}{2C}. \tag{9}$$

Here n_{fm} is an effective valence of the binding sites, $n_f = \sum_m n_{fm}$. We are free to choose any available approximation for $\mathcal{E}$, including those of [53, 59, 78]. One would not expect a difference in qualitative behaviour when choosing a different interaction, and this is demonstrated in [71]. Thus, without experimental evidence to the contrary, we choose (9) because it provides a simple and physically appealing interpretation of $\mathcal{E}$ by analogy with quantum dots [79, 80].

A subset of the calculated lowest energy levels is shown in Fig. 2 as a function of n_f. Each curve is parabolic and has a minimum when the total charge within the pore is neutralised ($Q = 0$). These minima correspond to *non-conducting* ground states of the SF that hold 0, 1, 2, or 3 potassium ions as shown by arrows.

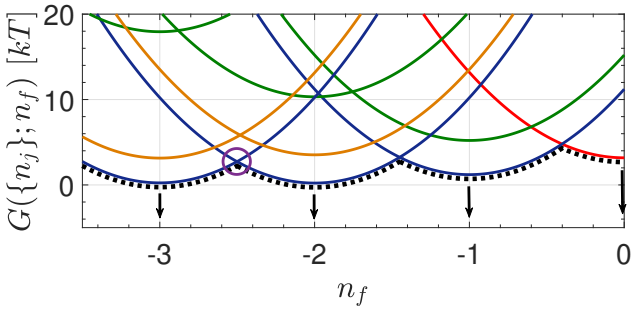

FIG. 2. Free energy *vs.* n_f with KCl and NaCl solutions at 0.2M. Only the most favoured states are included. Colours, red, blue, green, orange and black dashed denote empty, pure K^+ and Na^+, mixed and the ground states respectively. The purple circle shows when the pore is equally favourable to hold 2 or 3 K^+ ions. $\Delta\bar{\mu}_{K,1-4}$ in are $\sim 6.2, 5.7, 6, 6.2kT$ while $\Delta\bar{\mu}_{Na,1-4}$ are $\sim 2.2, -2.6, -1.6, 0.1kT$.

According to ICB theory, *conducting* states correspond to the degeneracies where the lowest energy levels intersect, cf. [53]. An example of this situation where 2-ion and 3-ion K^+ states are degenerate is highlighted by the purple circle. In accordance with MacKinnon's idea of charge balance [52], the total fixed charge is close to $Q_f = -2.5q$, corresponding to an average of 2.5 ions inside the pore. Assuming that all oxygen atoms are equally partially charged, we estimate their individual valences to be $z_0 \sim 0.125$ and find that the total charge on an 8-oxygen-caged binding site is $-1q$.

The vertical level-shifts are determined by the values $\Delta\bar{\mu}_{sm}$. These parameters are extracted through comparison with experimental data [11] and molecular dynamic simulations [32], including of the site's occupancies and current-voltage relations. Once the energy levels of the system states are known, we can calculate the occupancy and conductivity of each binding site and of the SF as a whole using Eqs. (4)-(7). The calculated multi-component SF occupancy and conductivity with mixed KCl and NaCl solutions are shown in Fig. 3.

In general, $\langle n_s \rangle$ and σ_s^T are complex multi-parametric surfaces. Here we plot their dependence on the selectivity (and affinity) of site S4 and n_f (see also [71]). Note the following key features. First, Eqs. (7) and (8) account for both the highly coordinated motion of ions in the channel (see Eqs. (29)-(37) of [71]) and the conductivity of individual sites in the presence of long range interactions. Secondly, the SF conductivity is smaller than the smallest site conductivity. Hence optimized conductance of the SF corresponds to nearly identical binding sites in line with experimental results. Thirdly, the whole SF becomes non-conducting when one site ceases to conduct. The SF conductivity resonates strongly as a function of both wall charge and $\Delta\bar{\mu}_{K,4}$. Therefore, a small change of parameters at a given site can inactivate the whole SF, thus illuminating a possible mechanism of C-type inacti-

vation [81].

The sensitive dependence of σ_T on its parameters suggests that the SF must be carefully tuned to achieve fast, strongly selective, diffusion of potassium ions. The corresponding optimal parameters can now be found analytically. As mentioned above, maximum conduction occurs when the sites share affinity and lowest energy levels intersect: $G(n_K+1,n_f)-G(n_K,n_f)\sim 0$, which is equivalent to equilibrium between the bulks and SF i.e. $\mu_s^b=\mu_s^c$ cf [53]. Note that we neglect a small entropy contribution from the fact that sites are now identical [71]. It follows directly that maximal conductivity occurs when,

$$\bar{\mu}_{Km}^{c,*}=\bar{\mu}_K^b+kT\ln(x_K)-\Delta\mathcal{E}-kT\ln[(n_K+1)/n_0], \quad (10)$$

Eq. (10) can be inverted to identify the optimal fixed charge for the SF. If we consider $n_f\sim -2.5$, and 0.2M solutions then we estimate $\Delta\bar{\mu}_{Km}^*\approx 6kT$, consistent with results from fitting.

The energy barrier to add Na^+ to site m, can be found from the conditions of maximal K^+ conductivity,

$$\Delta G_{Na}=G(n_K+n_{Na})-G(n_K)\sim\Delta\tilde{\mu}_{Km}-\Delta\tilde{\mu}_{Nam}, \quad (11)$$

which is equivalent to the Eisenman selectivity relation [43]. Note that we have neglected the entropic contributions due to mixing of ions and sites. Thus the theory resolves the long-standing conundrum [82] of simultaneous fast conduction with strong selectivity of the KcsA SF, and shows that Eisenman's strong selectivity relation follows directly from the condition of fast conduction.

An illustration is shown in Fig. 3. The state of the WT pore tuned for maximum conduction of K^+ ions and strong selectivity of K^+ over Na^+ is shown by the blue and red stars on the conductivity surfaces in the figure. The conductivity ratio $\sigma_K^{T,WT}/\sigma_{Na}^{T,WT}\sim 2\times 10^3$ is comparable with the commonly quoted ratio 1:1000 [42].

Because different points of the multi-parametric surfaces (Fig. 3) correspond to different experimental conditions (e.g. pH, concentrations) and mutations of the SF, the theory paves the way to detailed structure-function studies for many experimentally observed phenomena.

Next we apply the theory to the analysis of the T75C point mutation in the KcsA SF [11] replacing threonine with cysteine at location S4. This change does not significantly alter the side-chain volume but varies the electrostatic properties because the MuT lacks 4 hydroxyl ligands, lowering the total attractive charge of the filter. Experiment demonstrates that the distribution of K^+ ions in the SF is modified between the WT and MuT and that it conducts potassium at a lower rate.

To compare experimental results with theoretical predictions we take into account both the change in geometry and the fixed charge of the pore. The modified state of the system (green star in Fig. 3) corresponds to the reduced charge of the SF from -2.5q to -2.32q, reduced affinity of S4' from 6.2 to 5.2 kT, and volume change of

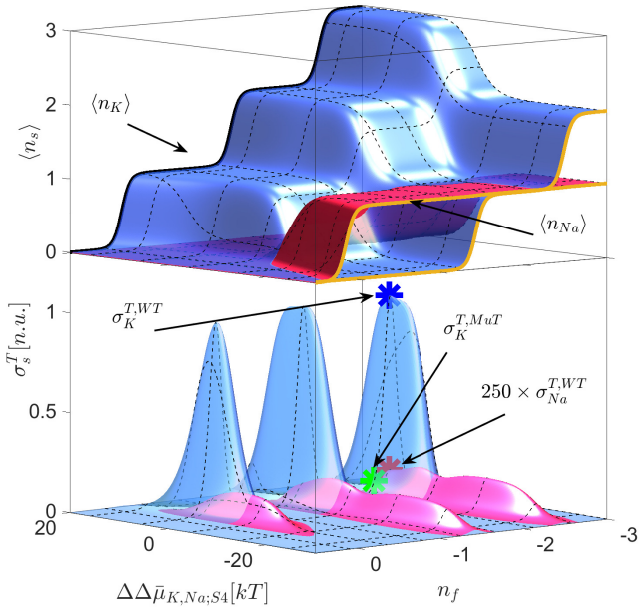

FIG. 3. K^+ (blue) and Na^+ (red) occupancy (top) and conductivity (bottom) *vs.* n_f and $\Delta\bar{\mu}_{K,Na;S4}$ in symmetrical 0.2M mixed bulk solutions. Conductivity and occupancy form a set of resonant peaks and steps respectively. Peaks maximise under the condition of barrier-less knock on, it being the favoured species and minimal difference in site affinity. Using identical parameters to Fig. 2, we indicate the WT K^+ (blue) and Na^+ (red) and MuT K^+ (green) conductivity's via coloured stars. Selectivity appears via the shift in both occupancy and conductivity from K^+ (blue) to Na^+ (red) surfaces, and the conductivity ratio yields $\sigma_K^{T,WT}/\sigma_{Na}^{T,WT}\sim 2\times 10^3$.

S4 by factor 1.2. The pore diffusivity in WT and MuT was estimated to be $2.3\times 10^{-10}\mathrm{m^2s^{-1}}$, which is less than the bulk value, as expected [19, 64]. Using the n_fs of the WT and MuT we can revise our earlier estimate, finding that the partial charge from each carbonyl group oxygen provides $-0.145q$ and the charge contribution from each hydroxyl group oxygens provide $-0.045q$.

The theoretical predictions are compared to experimental WT and MuT current-voltage data in Fig. 4 (a). The comparisons (extended beyond validity of the linear response regime) are shown with dashed lines. The reduced conduction in the mutant due to the increased resistivity of the S4' site (*vs.* S4 in the WT) can be clearly seen in the figure. The conductivity ratio $\sigma_K^{T,WT}/\sigma_K^{T,MuT}\sim 12.5$. Conduction via S1-S4 in the WT is almost barrier-less, corresponding to maximum conductivity while, for the mutant, an incoming ion faces an energy barrier of $\sim 4kT$ obstructing entry. Although this barrier is less than those observed in simulations [14], conduction in our theory is also inhibited by the loss in conductivity of S4'.

We note that similar results have been obtained experimentally for other KcsA mutants, e.g. with threonine at S4 replaced with alanine, decreasing conductance by a

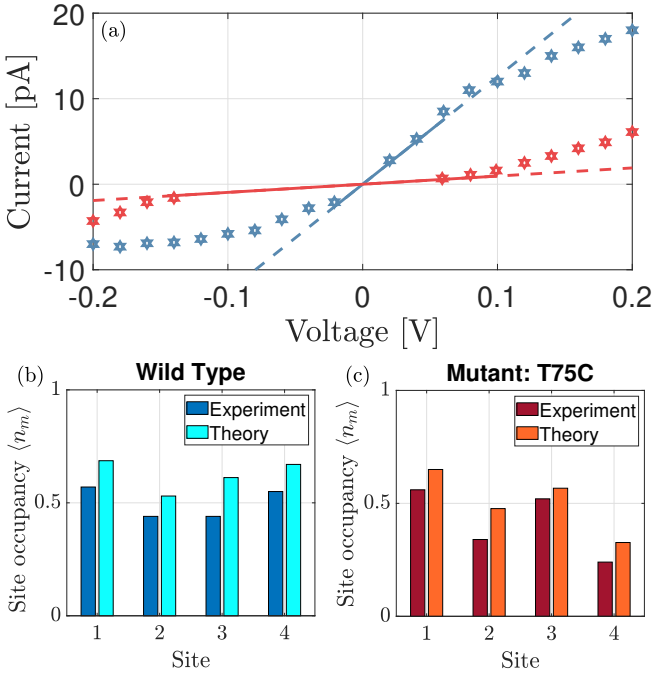

FIG. 4. Comparison of theoretical current (a) (lines), and site occupancy (b) and (c) to experimental data [11] denoted by stars in (a) and as labelled in (b) and (c). Theory and data are shown for the WT in blues and for the mutant (MuT) in reds. By comparison we find: $\Delta\bar{\mu}_{K,1-3} \sim 6.2, 5.7, 6kT$, $\Delta\bar{\mu}^{WT}_{K,4} \sim 6.2kT$ and $\Delta\bar{\mu}^{MuT}_{K,4} \sim 5.2kT$, a diffusivity in the channel of $2.3 \times 10^{-10}\mathrm{m}^2\mathrm{s}^{-1}$. The charge of the mutant was estimated as $n_f \sim -2.32$.

factor of $\sim$ 17 at the potential +100mV [15]. In addition, the second site, S2, has also been mutated [14] by substituting glycine with either alanine or cysteine, effectively removing S3, reducing occupancy of S1, and decreasing conduction by a factor of $\sim$ 32 at 200mV. We expect the theory to be applicable to these and a wide range of other point mutations.

Our statistical and linear response theory accounts quantitatively for ionic conduction and selectivity in the KcsA and mutant channels used as examples. It encompasses the geometry of individual sites, long range interactions, binding site affinities, bulk properties, and strongly correlated ionic motion in the SF. Thus, it provides a complex multi-dimensional map of the permeation properties of biological pores, including mutated pores. This is illustrated in Fig. 3 and examples in [71]. In KcsA, knock-on conduction is found to occur at almost the rate of free diffusion but with strong selection of K^+ over Na^+, in accord with experiments. This fast conduction requires the SF to have nearly identical binding sites, and optimal values of fixed charge and excess chemical potential at the sites. We find that the Eisenman relations of strong thermodynamic selectivity follow directly from the condition for fast conduction, thereby resolving analytically the long-standing *selectivity-conductivity paradox*. The theory may also offer insight into the recently-proposed 3-4 ion knock-on conduction mechanism [37, 38], the role of different Na^+-selective binding sites, and the differing transport properties of individual channels within the K^+-family. Furthermore, it provides the foundation for kinetic modelling [68] and can incorporate polarisation. We elaborate on these ideas, and more, in [71].

We acknowledge valuable discussions with Lewis Williamson, Ryan Hunt, Bob Eisenberg, Igor Khovanov and Aneta Stefanovska. The work was funded by a PhD Scholarship from the Faculty of Science and Technology of Lancaster University, by the UK Engineering and Physical Sciences Research Council (grants EP/M016889/1 and EP/M015831/1), and by a Leverhulme Trust Research Project Grant RPG-2017-134.

* w.gibby@lancaster.ac.uk
† dmitry.g.luchinsky@nasa.gov
‡ p.v.e.mcclintock@lancaster.ac.uk

[1] L. Wang, M. S. Boutilier, P. R. Kidambi, D. Jang, N. G. Hadjiconstantinou, and R. Karnik, Nat. Nanotechnol. **12**, 509 (2017).
[2] B. Hille, *Ion Channels Of Excitable Membranes* (Sinauer Associates, Sunderland, MA, 2001), 3rd ed.
[3] B. Roux, Essays Biochem. **61**, 201 (2017).
[4] M. S. Mauter, I. Zucker, F. Perreault, J. R. Werber, J.-H. Kim, and M. Elimelech, Nat. Sustain. **1**, 166 (2018).
[5] D. Deamer, M. Akeson, and D. Branton, Nat. Biotechnol. **34**, 518 (2016).
[6] F. M. Ashcroft, *Ion Channels and Disease* (Academic press, 1999).
[7] X. Huang and L. Y. Jan, J. Cell Biol. **206**, 151 (2014).
[8] D. J. Aidley and P. R. Stanfield, *Ion Channels: Molecules in Action* (CUP, Cambridge, 2000).
[9] S.-H. Chung, V. Krishnamurthy, and O. S. Andersen, *Biological Membrane Ion Channels Dynamics, Structure, and Applications* (Springer, 2007).
[10] L. Heginbotham, Z. Lu, T. Abramson, and R. MacKinnon, Biophys. J. **66**, 1061 (1994).
[11] M. Zhou and R. MacKinnon, J. Mol. Biol. **338**, 839 (2004).
[12] M. Derebe, D. Sauer, W. Zeng, A. Alam, N. Shi, and Y. Jiang, Proc. Nat. Acad. Sci. (USA) **108**, 598 (2011).
[13] V. Oakes, S. Furini, and C. Domene, J. Chem. Theo. Comput. **16**, 794 (2020).
[14] C. Tilegenova, D. M. Cortes, N. Jahovic, E. Hardy, P. Hariharan, L. Guan, and L. G. Cuello, Proc. Nat. Acad. Sci. (USA) **116**, 16829 (2019).
[15] A. J. Labro, D. M. Cortes, C. Tilegenova, and L. G. Cuello, Proc. Nat. Acad. Sci. **115**, 5426 (2018).
[16] D. Naranjo, H. Moldenhauer, M. Pincuntureo, and I. Díaz-Franulic, Journal of General Physiology **148**, 277 (2016).
[17] D. Bucher, S. Raugei, L. Guidoni, M. Dal Peraro, U. Rothlisberger, P. Carloni, and M. L. Klein, Biophys. Chem. **124**, 292 (2006).
[18] S. Kraszewski, C. Boiteux, C. Ramseyer, and C. Gi-

rardet, Phys. Chem. Chem. Phys. **11**, 8606 (2009).
[19] D. P. Tieleman, P. C. Biggin, G. R. Smith, and M. S. P. Sansom, Quart. Rev. Biophys. **34**, 473 (2001).
[20] C. N. Schutz and A. Warshel, Proteins **44**, 400 (2001).
[21] J. A. Ng, T. Vora, V. Krishnamurthy, and S.-H. Chung, Eur. Biophys. J. **37**, 213 (2008).
[22] S. Varma and S. B. Rempe, Biophys. J. **99**, 3394 (2010).
[23] S. Varma, D. M. Rogers, L. R. Pratt, and S. B. Rempe, J. Gen. Physiol. **137**, 479 (2011).
[24] D. Bucher and U. Rothlisberger, J. Gen. Physiol. **135**, 549 (2010).
[25] S. De, C. Rinsha, A. Joseph, A. Ben, V. Krishnapriya, et al., Phys. Chem. Chem. Phys. **20**, 17517 (2018).
[26] G. Lamoureux, A. D. MacKerell Jr, and B. Roux, The Journal of chemical physics **119**, 5185 (2003).
[27] G. Lamoureux and B. Roux, The Journal of chemical physics **119**, 3025 (2003).
[28] J. A. Lemkul, J. Huang, B. Roux, and A. D. MacKerell Jr, Chemical reviews **116**, 4983 (2016).
[29] V. Ngo, H. Li, A. D. MacKerell Jr, T. W. Allen, B. Roux, and S. Noskov, Journal of Chemical Theory and Computation (2021).
[30] A. Thompson, I. Kim, T. Panosian, T. Iverson, T. Allen, and C. Nimigean, Nat. Struct. Mol. Biol. **16**, 1317 (2009).
[31] C. Nimigean and T. Allen, J. Gen. Physiol. **137**, 405 (2011).
[32] I. Kim and T. W. Allen, Proc. Nat. Acad. Sci. (USA). **108**, 17963 (2011).
[33] C. M. Nimigean and C. Miller, J. Gen. Physiol. **120**, 323 (2002).
[34] D. Medovoy, E. Perozo, and B. Roux, Biochim. Biophys. Acta (BBA) – Biomembranes **1858**, 1722 (2016).
[35] D. Doyle, J. Cabral, R. Pfuetzner, A. Kuo, J. Gulbis, S. Cohen, B. Chait, and R. MacKinnon, Science **280**, 69 (1998).
[36] J. Morais-Cabral, Y. Zhou, and R. MacKinnon, Nature **414**, 37 (2001).
[37] D. Köpfer, C. Song, T. Gruene, G. Sheldrick, U. Zachariae, and B. de Groot, Science **346**, 352 (2014).
[38] W. Kopec, D. A. Köpfer, O. N. Vickery, A. S. Bondarenko, T. L. Jansen, B. L. de Groot, and U. Zachariae, Nat. Chem. **10**, 813 (2018).
[39] M. Barabash, W. A. T. Gibby, C. Guardiani, D. Luchinsky, and P. V. E. McClintock, Fluct. Noise Lett. **18**, 1940006 (2019).
[40] Y. Liu and F. Zhu, Biophys. J. **104**, 368 (2013).
[41] T. Sumikama and S. Oiki, J. Physiol. Sci. **69**, 919 (2019).
[42] L. Coates, Acta Crystallogr. D **76**, 326 (2020).
[43] G. Eisenman and R. Horn, J. Membrane Biol. **76**, 197 (1983).
[44] F. Bezanilla and C. Armstrong, J. Gen. Physiol. **60**, 588 (1972).
[45] D. Gillespie and R. Eisenberg, Euro. Biophys. J. **31**, 454 (2002).
[46] D. Gillespie, W. Nonner, D. Henderson, and R. S. Eisenberg, Phys. Chem. Chem. Phys. **4**, 4763 (2002).
[47] D. Gillespie, W. Nonner, and R. S. Eisenberg, Phys. Rev. E **68**, 031503 (2003).
[48] D. Boda, W. Nonner, D. Henderson, B. Eisenberg, D. Gillespie, et al., Biophys. J. **94**, 3486 (2008).
[49] D. Gillespie, L. Xu, and G. Meissner, Biophy. J. **107**, 2263 (2014).
[50] A. Hodgkin and R. Keynes, J. Physiol. **128**, 61 (1955).
[51] S. Berneche and B. Roux, Nature **414**, 73 (2001).
[52] Y. Zhou and R. MacKinnon, J. Mole. Biol. **333**, 965 (2003).
[53] S. Yesylevskyy and V. Kharkyanen, Chem. Phys. **312**, 127 (2005).
[54] V. N. Kharkyanen, S. O. Yesylevskyy, and N. M. Berezetskaya, Phys. Rev. E **82**, 051103 (2010).
[55] M. Krems and M. Di Ventra, J. Phys. Condens. Matter **25**, 065101 (2013).
[56] I. K. Kaufman, D. G. Luchinsky, R. Tindjong, P. V. E. McClintock, and R. S. Eisenberg, Phys. Biol. **10**, 026007 (2013).
[57] I. K. Kaufman, P. V. E. McClintock, and R. S. Eisenberg, New J. Phys. **17**, 083021 (2015).
[58] J. Zhang, A. Kamenev, and B. I. Shklovskii, Phys. Rev. Lett. **95**, 148101 (2005).
[59] J. Zhang, A. Kamenev, and B. I. Shklovskii, Phys. Rev. E **73**, 051205 (2006).
[60] J. Feng, K. Liu, M. Graf, D. Dumcenco, A. Kis, M. Di Ventra, and A. Radenovic, Nat. Mater. **15**, 850 (2016).
[61] N. Kavokine, S. Marbach, A. Siria, and L. Bocquet, Nat. Nanotechnol. **14**, 573 (2019).
[62] B. Roux, Biophys. J. **77**, 139 (1999).
[63] W. Im, S. Seefeld, and B. Roux, Biophys. J. **79**, 788 (2000).
[64] B. Roux, T. Allen, S. Berneche, and W. Im, Quart. Rev. Biophys. **37**, 15 (2004).
[65] D. M. Rogers, T. L. Beck, and S. B. Rempe, J. Stat. Phys. **145**, 385 (2011).
[66] I. K. Kaufman, O. A. Fedorenkon, D. G. Luchinsky, W. A. Gibby, S. K. Roberts, P. V. E. McClintock, and R. S. Eisenberg, EPJ Nonlin. Biomed. Phys. **5**, 4 (2017).
[67] W. Nonner, D. P. Chen, and B. Eisenberg, Biophys. J. **74**, 2327 (1998).
[68] W. A. T. Gibby, M. L. Barabash, C. Guardiani, D. G. Luchinsky, O. A. Fedorenko, S. K. Roberts, and P. V. E. McClintock, Fluct. Noise Lett. **18**, 1940007 (2019).
[69] L. G. Cuello, D. M. Cortes, and E. Perozo, Elife **6**, e28032 (2017).
[70] E. F. Pettersen, T. D. Goddard, C. C. Huang, G. S. Couch, D. M. Greenblatt, E. C. Meng, and T. E. Ferrin, J. Comput. Chem. **25**, 1605 (2004).
[71] SUPPLEMENTAL MATERIAL for this paper (2020).
[72] B. Widom, J. Phys. Chem. **86**, 869 (1982).
[73] D. Gillespie, Biophys. J. **94**, 1169 (2008).
[74] J. G. Kirkwood, J. Chem. Phys. **3**, 300 (1935).
[75] L. D. Landau and E. M. Lifshitz, *Statistical Physics. Course of Theoretical Physics.* Volume 5. Third edition, Part I (Pergamon Press, Oxford, 1980).
[76] D. A. Chesnut and Z. W. Salsburg, J. Chem. Phys. **38**, 2861 (1963).
[77] A. P. Hughes, U. Thiele, and A. J. Archer, Am. J. Phys. **82**, 1119 (2014).
[78] E. Kitzing, in *Membrane Proteins: Structures, Interactions and Models:* Proc. 25th Jerusalem Symposium on Quantum Chemistry and Biochemistry, Jerusalem, May 18-21,1992, edited by A. Pullman, J. Jortner, and B. Pullman (Springer Netherlands, Dordrecht, 1992), pp. 297–314.
[79] C. Beenakker, Phys. Rev. B **44**, 1646 (1991).
[80] E. Bonet, M. M. Deshmukh, and D. Ralph, Physical Review B **65**, 045317 (2002).
[81] Y. Xu and A. E. McDermott, J. Struct. Biol. X **3**, 100009 (2019).
[82] R. Horn, B. Roux, and J. Åqvist, Biophys. J. **106**, 1859

(2014).